J Comp Physiol A (1986) 158:795–811

Journal of Comparative Physiology A Sensory, Neural, and Behavioral Physiology

Electrical coupling of neuro-ommatidial photoreceptor cells in the blowfly

J.H. van Hateren

Department of Biophysics, Laboratory for General Physics, University of Groningen, Westersingel 34, NL-9718 CM Groningen, The Netherlands

Accepted March 17, 1986

Summary. A new method of microstimulation of the blowfly eye using corneal neutralization was applied to the 6 peripheral photoreceptor cells (R1–R6) connected to one neuro-ommatidium (and thus looking into the same direction), whilst the receptor potential of a dark-adapted photoreceptor cell was recorded by means of an intracellular microelectrode. Stimulation of the photoreceptor cells not impaled elicited responses in the recorded cell of about 20% of the response elicited when stimulating the recorded cell. This is probably caused by gap junctions recently found between the axon terminals of these cells. Stimulation of all 6 cells together yielded responses that were larger and longer than those obtained with stimulation of just the recorded cell, and intensity-response curves that deviated more strongly from linearity. Evidence is presented that the resistance of the axon terminal of the photoreceptor cells quickly drops in response to a light flash, depending on the light intensity. Incorporating the cable properties of the cell body and the axon, the resistance of the gap junctions, and the (adapting) terminal resistance, a theoretical model is presented that explains the measurements well. Finally, it is argued that the gap junctions between the photoreceptor cells may effectively uncouple the synaptic responses of the cells by counteracting the influence of field potentials.

Introduction

Fly photoreceptor cells R1–R6 that look into the same direction are coupled to each other by gap junctions between their axon terminals (Chi and Carlson 1976; Ribi 1978; Shaw and Stowe 1982). These gap junctions couple the terminals electrically (Shaw 1984b). In the present article this coupling is investigated with a novel technique for stimulating the eye, with which photoreceptors can be stimulated individually under visual control.

The compound eye of the blowfly is a neural superposition eye (Kirschfeld and Franceschini 1968), see Fig. 1. An eye consists of a few thousand ommatidia, each with its own facet lens. Behind each lens 8 photoreceptors (rhabdomeres) are arranged such, that 8 photoreceptors behind different lenses look into the same direction. These 8 photoreceptor cells have their axons going to the same cartridge (or neuro-ommatidium) in the first

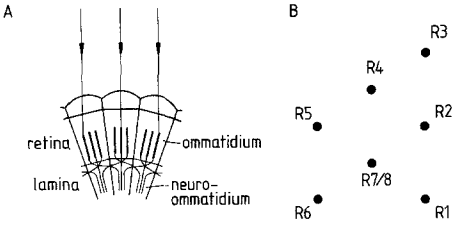

Fig. 1. A The fly's eye consists of ommatidia, each having its own facet lens and 8 photoreceptors (rhabdomeres), of which 3 are shown in the figure. The photoreceptors of one ommatidium have different receptive fields, but they share their receptive field with several rhabdomeres in neighbouring ommatidia. In the figure this is shown for 3 rhabdomeres: they receive light from a common direction. The axons of the photoreceptor cells that look into the same direction all project to the same column in the lamina. Thus these columns, called neuro-ommatidia, receive only input from one direction in space, contrary to the ommatidia. The axons of the photoreceptors R1–R6 synapse on second order neurons in the lamina, whereas the axons of R7 and R8 pass the lamina to the next neuropil (the medulla). **B** The photoreceptors in an ommatidium form a pattern as shown (see also Fig. 3). The outer rhabdomeres, R1–R6, project to 6 different neuro-ommatidia in the lamina. The tiered, central two rhabdomeres, R7 and R8, project to the medulla

neuropil, the lamina. There 6 of them, R1–R6, superimpose on second order neurons.

In natural circumstances the 6 coupled cells are all stimulated simultaneously, because they receive light from the same direction in space. Most studies on the receptor potential of fly photoreceptor cells have been performed therefore with illumination of the 6 coupled cells. The responses have commonly been interpreted, however, as originating exclusively from the recorded cell. We will see that this is not the case: the response is also determined by the other photoreceptor cells looking into the same direction. Moreover, we will see that changes in the axon terminals in the lamina also shape the responses in the cell body.

To help interpreting these findings a quantitative model is presented that describes the transport of the light-evoked signal from the sense cells to the lamina. One of the surprising outcomes of this study is that the gap junctions between the photoreceptor cells may effectively uncouple the synaptic responses of the cells by counteracting the influence of field potentials.

Methods

Animals and preparation. Experiments were performed on females of the blowfly, *Calliphora erythrocephala* (wild type). About 40 animals were used for this study. The animals were fixed with wax and mounted on a goniometer. A hole was made at the back side of the head by removing a small piece of chitin, and a small plastic light guide was inserted through this hole for antidromic illumination. A small piece of the cornea was also removed, and a microelectrode inserted, which impaled cells in the frontal region of the eye, in the retina or the lamina depending on the angle of insertion of the electrode. The indifferent electrode was placed ipsilaterally in an unstimulated part of the retina. The flies were dark adapted for at least 45 min.

Electrophysiology. Conventional glass microelectrodes were used, filled with a mixture of 3 *M* KAc and 0.1 *M* KCl, and having a typical resistance of 150 MΩ measured in 150 m*M* NaCl. Electrodes of slightly lower resistance (100–120 MΩ) were used for injecting current, because they had better current-voltage characteristics. For current injection the capacity compensation of the amplifier (Muijser 1979) was adjusted just below instability, which yielded rise times of 0.3 ms. The obtained measurements (e.g. Fig. 10) were corrected for this delay by shifting them 0.3 ms backwards. Coarse balancing of the microelectrode resistance was done by adjusting the balance of the amplifier; the remaining imbalance in the averaged measurements was corrected by computer. Recordings from the axon were identified as coming from the axon terminal, when lamina monopolar cells were impaled before and after impalement of the axon.

Optical setup. Lenses L_1, L_2 and L_3 (see Fig. 2) form together a waterimmersion microscope, L_2 is a field lens. Light coming from a lightguide inserted in a hole at the back of the head of the fly propagates through the rhabdomeres (functioning as lightguides) towards this microscope. The waterimmersion neutralizes the cornea (Franceschini 1975), so that we can see the rhabdomeres beneath the corneal lenses. The light coming from the eye is partially reflected by the pellicle half-mirror *P* to a microscope and an image intensifier. There we can see the rhabdomeres together with the stimulus, which is partially imaged on the rhabdomeres, and partially reflected at the pellicle, reflected by the mirror *M*, and transmitted through the pellicle to the microscope and the image intensifier. The position of the stimulus relative to the rhabdomeres as seen by the observer is identical to the real image of the stimulus on the rhabdomeres: this is due to the design of the instrument (see van Hateren 1985). The stimulus consisted of LEDs (Siemens LD57C) having a spectral peak at 560 nm with a half-width of 25 nm. They were mounted on small magnets that could be placed anywhere in the visual field on an iron plate. Antidromic light of 600 nm was used when looking with the naked eye. This has the drawback that it light adapts the photoreceptors. Therefore, usually light of 700 nm was used together with the image intensifier.

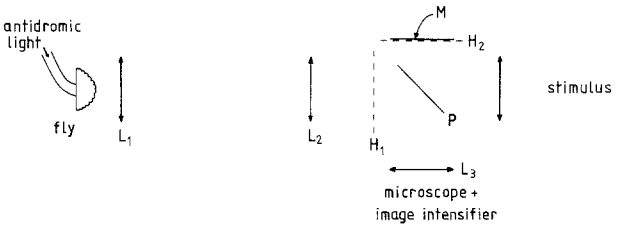

Fig. 2. Optical setup for stimulating single rhabdomeres. Light propagates through a small lightguide into the back of the head of the fly, through the rhabdomeres (acting as lightguides), and towards the waterimmersion microscope consisting of lenses L_1 (Leitz 1,00 50:1), L_2 (doublet, f=60 mm), and L_3 (Photar, f=25 mm). The stimulus is imaged onto the rhabdomeres, but it can also be seen through the microscope and image intensifier because its light is partially reflected by the pellicle *P*, the mirror *M*, and transmitted through the pellicle to the microscope and image intensifier (Oldelft XX1136). Rhabdomeres and stimulus are imaged in the plane H_1, the stimulus also in plane H_2. The rhabdomeres are seen in plane H_1, and the stimulus in plane H_2, which is coplanar with the reflection of plane H_1 by the pellicle

Stimulus generation and data acquisition. Both stimulus generation and data acquisition were performed by a Data General Desktop 20 microcomputer. Stimulus generation was done by a laboratory-built 15-channel DAC. Each channel could drive a voltage-driven current source driving a LED. The DAC had buffers for each channel to give the LEDs a new intensity simultaneously. The intensity of each LED was measured as a function of DAC voltage, and stored in a file in the computer. This file was used for the stimulus generation to obtain well-defined intensities. We note that the responses of different sense cells to a given intensity can not be strictly compared, because the sensitivity and the latency of the cells varies somewhat. Most experiments were done with 500 ms between successive stimuli; this did not cause appreciable light adaptation for responses up to several mV, as control experiments with longer times between successive stimuli showed.

The potentials recorded were amplified and sampled by an ADC. The ADC and DAC were driven synchronously by the same clock, usually at 1 kHz, both using direct memory access. For the current injection experiment of Fig. 10 the cur-

rent source in the amplifier was also driven by the DAC, but in this case the ADC was driven by a 10 kHz clock (synchronized with the DAC). No prefiltering was used before sampling the signal with the ADC, because this proved to be unnecessary. Aliasing is not a real problem, because the photoreceptor cells act themselves as effective low-pass filters. Furthermore, the extra delay (and distortion) in the signal introduced by prefiltering was considered disadvantageous for the measurements presented here.

The responses were averaged on line and displayed on a graphics terminal. The data were also stored on a Winchester disk for off-line analysis. These data were afterwards transferred to a DG Eclipse minicomputer for further processing and storage on magnetic tape. Averaged data were sent to a Cyber 170/760 mainframe for analysis with the help of the theoretical model presented in the Appendix.

Results

The method of microstimulation

The optical method of stimulating individual photoreceptors is demonstrated by Fig. 3, a photograph of what we can see through the equipment used for stimulation (Fig. 2). Light propagates antidromically through the eye, and waterimmersion neutralizes the cornea, thus the rhabdomere tips are directly visible. The 6 brighter dots are the LEDs used as stimuli. They are imaged on the rhabdomeres R1–R6 that belong to one neuro-ommatidium and that thus would be looking into the same direction if the cornea were not neutralized. On impalement of a photoreceptor cell illumination of its rhabdomere produces much larger responses than stimulation of all other photoreceptors (at least if no artificial coupling is induced by the microelectrode; see Smakman 1985). This identifies the sense cell impaled.

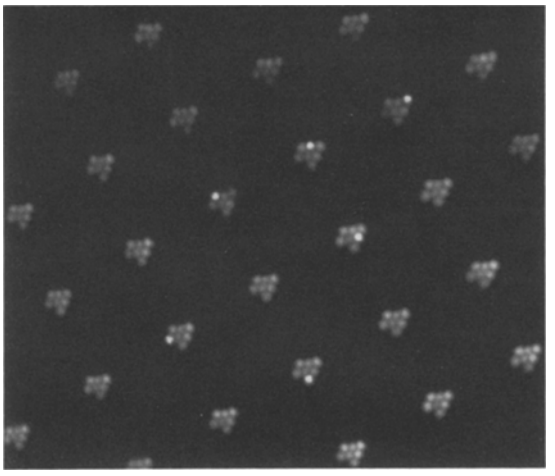

Fig. 3. A photograph of what can be seen through the optical setup described in Fig. 2. Several ommatidia are seen, each with a group of 7 waveguides (which are seen as bright dots), the outer ones being the rhabdomeres R1–R6, the central one consisting of the tiered rhabdomeres R7 and R8. The lenses in front of these groups are neutralized by waterimmmersion. The 6 brightest dots are LEDs imaged onto rhabdomeres R1–R6 that would receive light coming from the same direction if the cornea were not neutralized

Recordings from the cell body

Illumination of other sense cells, in particular those going to the same neuro-ommatidium as the recorded cell, may also cause (smaller) depolariza-

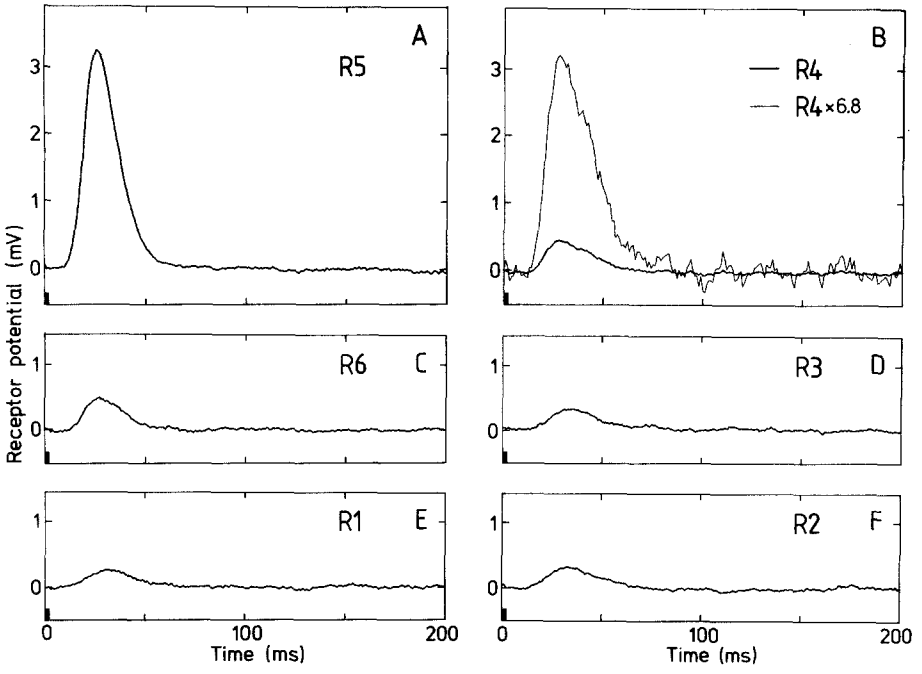

Fig. 4. Examples of receptor potentials obtained from an R5 when stimulating this R5 (**A**) and other cells looking into the same direction (**B–F**). The stimulus consisted of light flashes of 2 ms (black bars at the bottom left of each figure) of intensity 10 (arbitrary units). Each response is the average of 160 flashes. In **B** there is also a rescaled response (thin line) to enable comparison of the shape of the response to **A**

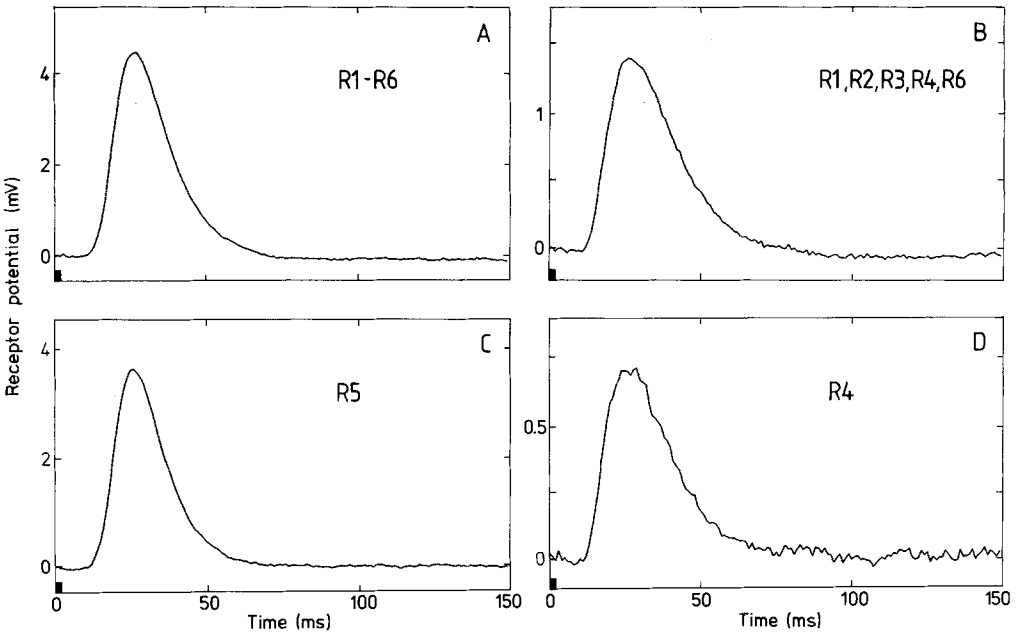

Fig. 5A–D. Examples of responses of the same cell as in Fig. 4 for various stimuli of intensity 13. In **C** only the recorded cell was stimulated, in **A** all cells, in **D** one neuro-ommatidial neighbour, and in **B** all neuro-ommatidial neighbours. Responses are averages of 160 flashes

tions (Shaw 1981, 1984b). Figure 4 shows an example of the responses to short (2 ms) light flashes. An R5 was impaled here, as was inferred from the stimulus position necessary for maximal response. Illumination of the neuro-ommatidial neighbours (other sense cells connected to the same neuro-ommatidium) also depolarized the R5. In Fig. 4B the response was rescaled to enable comparison to Fig. 4A. The response to illumination of R4 is somewhat broader than the response to illumination of R5, as is the case for the responses shown in Fig. 4C, D, E and F. In general, illumination of photoreceptor cells further away from the recorded cell in the ring of terminals (see below), yielded slightly smaller and slower responses.

Two possible explanations of these depolarizations, stray light and field potentials in the retina, were examined and discarded. Stray light can be ruled out because light flashes from a LED imaged not on a rhabdomere but between the rhabdoms elicited no response. Field potentials can be ruled out because illumination of a different photoreceptor in the ommatidium of a neuro-ommatidial photoreceptor (for example illumination of R6 in the ommatidium of the R4 of Fig. 4) gave negligible responses in the recorded cell, but must have produced comparable field potentials as illumination of the neuro-ommatidial photoreceptor. This control experiment also rules out stray light produced by re-radiation from excited rhabdomeres (Shaw 1984b) as the source of the depolarizations. A likely explanation of the responses is the fact that the axons of the neuro-ommatidial visual sense cells are coupled to each other by gap junctions in the lamina, chiefly between next-neighbours in the ring of terminals, cyclically arranged in the order R1–R2–R3–R4–R5–R6 (Chi and Carlson 1976; Ribi 1978; Shaw and Stowe 1982). The response in an illuminated cell is then propagated to the lamina, partially transmitted through the gap junctions to neighbouring neuro-ommatidial sense cells (and thereupon to next-next-neighbours, etc.), and propagated back to the cell bodies in the retina.

Figure 5 shows responses of a recorded R5 to various stimuli, all consisting of 2 ms light flashes. Responses to illumination of one neuro-ommatidial neighbour (Fig. 5D) and all neuro-ommatidial neighbours (Fig. 5B) are clearly broader than to illumination of R5 itself (Fig. 5C). Illuminating all 6 neuro-ommatidial sense cells (Fig. 5A) yields a response larger and slightly broader than illuminating just R5. The peak response amplitude to these stimuli is shown in Fig. 6 as a function of intensity. This measurement is a typical example taken from totally 12 identical measurements in different cells, all yielding very similar results (data from another cell are shown in Fig. 14, curves a and b). Comparing curves a and b of Fig. 6, we see that the response to illumination of 6 cells is

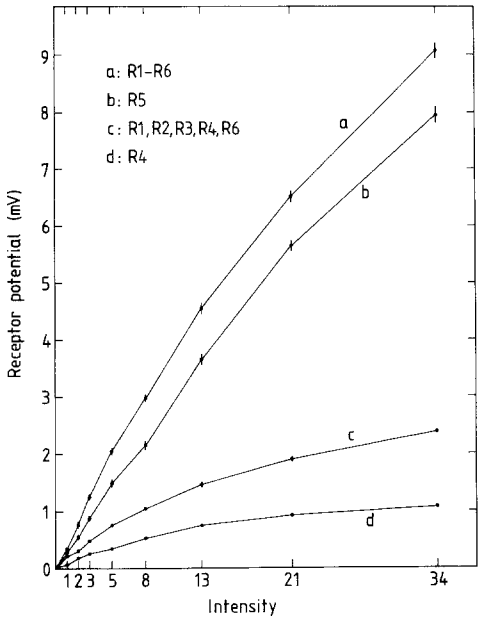

Fig. 6. Peak response amplitude for various stimuli as a function of the intensity of the light flash (again 2 ms). Data from the same cell as in Figs. 4 and 5. Measurements at intensity 13 are the same as the measurements of Fig. 5. Responses are averages of 160 flashes. Error bars show standard errors of the mean. Where no bars are visible, they have about the size of the filled circles. Note that both axes are scaled linearly. Stimuli for each curve consisted of 160 runs, where in each run the order of stimulus presentation was: intensities 5, 21, 2, 34, 8, 3, 1, 13. First, 160 runs were presented with alternatingly stimuli a and b, then 160 runs with alternatingly stimuli c and d

always larger than the response to illumination of the recorded cell. Furthermore, the relative difference between curves a and b becomes smaller for higher flash intensities: for low intensities the response to illumination of 6 cells is about 30% higher than the response to illumination of the recorded cell, whereas for the highest intensities this is only 15% or less. A consequence of this is that the curves have a somewhat different shape: curve b (illumination of the recorded cell) is more linear than curve a (illumination of 6 cells). This was consistently the case for all photoreceptor cells where these curves were measured, at least for responses up to several mV. In one experiment where responses up to 30 mV were induced by light flashes of 10 ms, the difference between illumination of 6 cells and 1 cell became a constant of about 1 mV for depolarizations larger than about 5 mV; thus the curves were approximately parallel for these larger depolarizations. Finally, if we compare curves b and d of Fig. 6 (illumination of the recorded cell and one of its neuro-ommatidial neighbours, respectively), we see that at low intensities a larger proportion of the response is transferred to a neighbouring cell than at high intensities. We assume here that both cells, R5 in curve b and R4 in curve d, give equal responses to equal stimuli. This will be only approximately true, because the sensitivity varies somewhat from cell to cell. The same restriction applies to the exact shape of the responses, and to their latency.

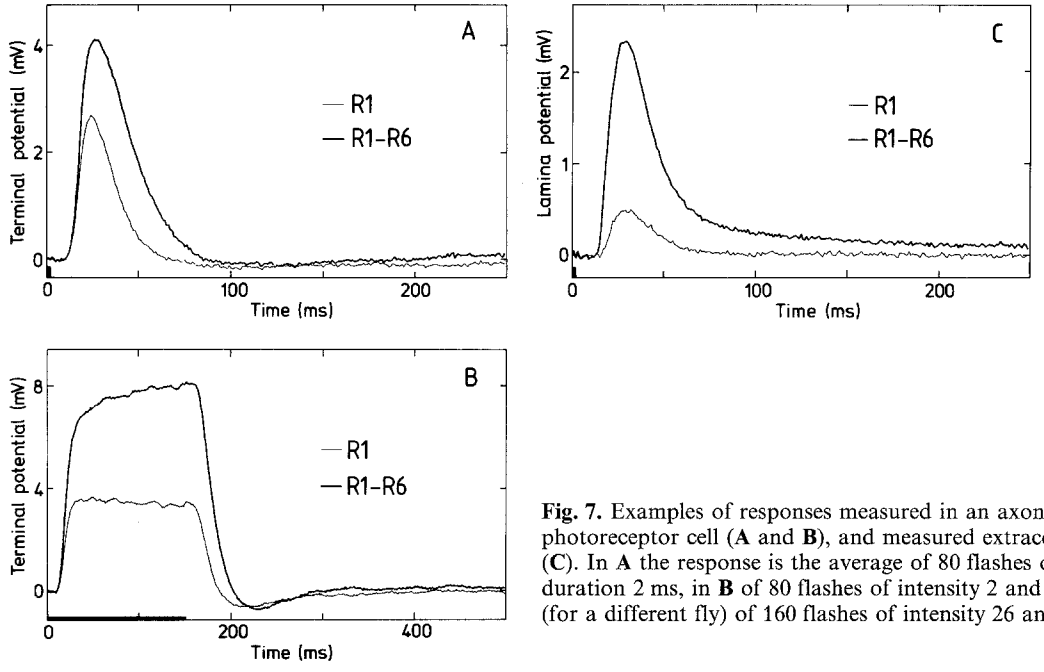

Fig. 7. Examples of responses measured in an axon terminal of a photoreceptor cell (**A** and **B**), and measured extracellularly in the lamina (**C**). In **A** the response is the average of 80 flashes of intensity 5 and duration 2 ms, in **B** of 80 flashes of intensity 2 and duration 150 ms, in **C** (for a different fly) of 160 flashes of intensity 26 and duration 2 ms

Recordings from the terminal and the lamina

Because the gap junctions are situated between the axon terminals of the sense cells in the lamina, it was suspected that the coupling that could be measured between the sense cells might be stronger in the terminals than in the cell bodies. This proved to be the case. An example is shown in Fig. 7A, where a terminal of an R1 was impaled. The difference between illumination of the recorded cell and the 6 coupled cells is larger than what was found in the cell bodies. Moreover, we found that illumination of one photoreceptor may elicit responses in a neuro-ommatidial neighbour of up to 50% of the response in the illuminated photoreceptor (this compares to 20–25% in the cell bodies). Not only the response height is different, also the pulse shape: illumination of 6 cells gives broader responses than illumination of the recorded cell; this effect is even stronger in the terminal than in the cell body.

Figure 7B shows responses to light stimuli of 150 ms. Apart from the height of the response the shapes are again slightly different: with illumination of 6 cells the response continues to rise somewhat during the light pulse, whereas with illumination of the recorded cell the response decreases slightly. Similar differences, but less pronounced, were measured in the cell body. Furthermore, we see in Fig. 7B that both responses have an undershoot at light-off. Again, a similar undershoot that can be measured in the cell body is less pronounced.

The lamina extracellular space may give remarkably large depolarizations in response to illumination (Shaw 1975). Figure 7C shows an example of responses that are probably extracellular (this is difficult to verify, however; it was concluded here from the noise characteristics of the responses). In this case the response to illumination of the 6 coupled cells is much larger than the response to illumination of the recorded cell (the ratio is here about 5:1, but this varies from measurement to measurement, possibly depending on the exact position of the microelectrode). Moreover, a depolarizing afterpotential develops. The peak response amplitudes of the terminal depolarization and the lamina extracellular depolarization are shown in Figs. 8 and 9 as a function of intensity.

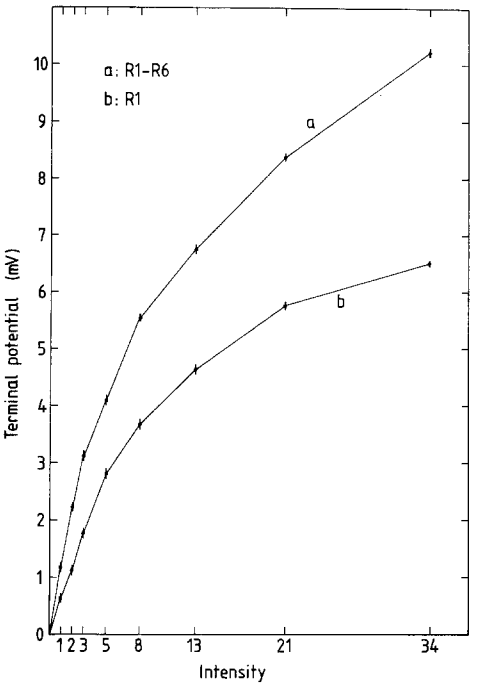

Fig. 8. Response height in an axon terminal (the same as in Fig. 7A) as a function of the intensity of the light flash (2 ms duration). Responses are averages of 80 flashes, error bars show standard errors of the mean. Order of stimulus presentation as in Fig. 6

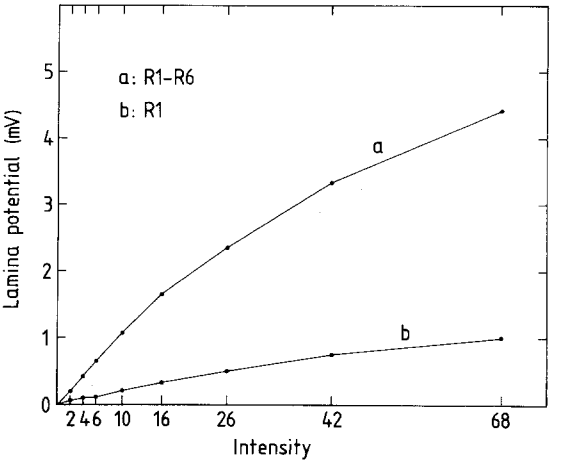

Fig. 9. Response height measured in the lamina extracellular space (the same as in Fig. 7C) as a function of the intensity of light flashes of 2 ms duration. Responses are averages of 160 flashes, standard errors of the mean fall within the filled circles. Order of stimulus presentation for each of the 160 runs: intensities 10, 42, 4, 68, 16, 6, 2, 26

Resistance measurements

In order to understand better what happens in these coupled photoreceptors we constructed a theoretical model for this system (see the Discussion). Necessary for this model were the electrical properties of the visual sense cell. Therefore, current pulses were injected in the cell body, which yielded information about the input impedance of the cell (Fig. 10). From measurements as that of Fig. 10

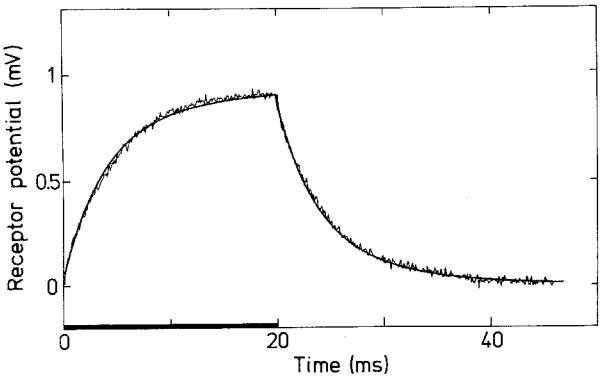

Fig. 10. Response to current injection in the cell body of a photoreceptor cell. Current pulses of 26.5 pA were injected during 20 ms (black bar). Responses to 1,280 pulses, sampled at 10 kHz, were averaged (thin line). The thick line is a theoretical fit to the data (see Discussion; gap resistance 70 MΩ, terminal resistance 1,000 MΩ, membrane area of the rhabdomere 35 $\mu m^2/\mu m$, membrane resistance 8 $k\Omega cm^2$, resulting input resistance 34.5 MΩ). The measurement was shifted by 0.3 ms to the left to correct for the rise time of the current pulse, and the voltage jump caused by the electrode resistance was subtracted (first electronically by the amplifier, second by computer). The voltage subtracted was adjusted until the voltage became continuous before and after current jumps. At 20 ms the overshoot caused by the rise time of the current pulse (3 data points) is not shown

input resistances of 25–35 MΩ were found (similar to what Hardie et al. 1981 report), and time constants of 5–8 ms (where we approximate the charging curve to an exponential). Hyperpolarizing current pulses yielded virtually identical values.

In a second experiment a train of current pulses was given in combination with a short light flash on the 6 coupled photoreceptors (Fig. 11A). Figure 11B shows the response to only the light flash, and Fig. 11C the difference between the curves of Fig. 11A and B. What remains is the response to the current pulses, which shows the dynamics of the cell's input resistance and time constant during the response to light. We assume here that the photocurrent is not influenced by the current pulses applied through the microelectrode; that is reasonable, because the voltage variations caused by the current pulses are much smaller than the voltage variation caused by the light stimulus. Looking first at the later part of the curve in Fig. 11C, we see that the cell is simply charged alternatively positive and negative. At the beginning of the curve, however, some dramatic differences arise. During the first (positive) current pulse the potential rises as expected, but then, as the light response reaches a few mV, the charging of the cell stops and even reverses (arrow)! This reversal takes place within 1 ms, the sample interval in this experiment. The response to the next (negative) current pulse shows

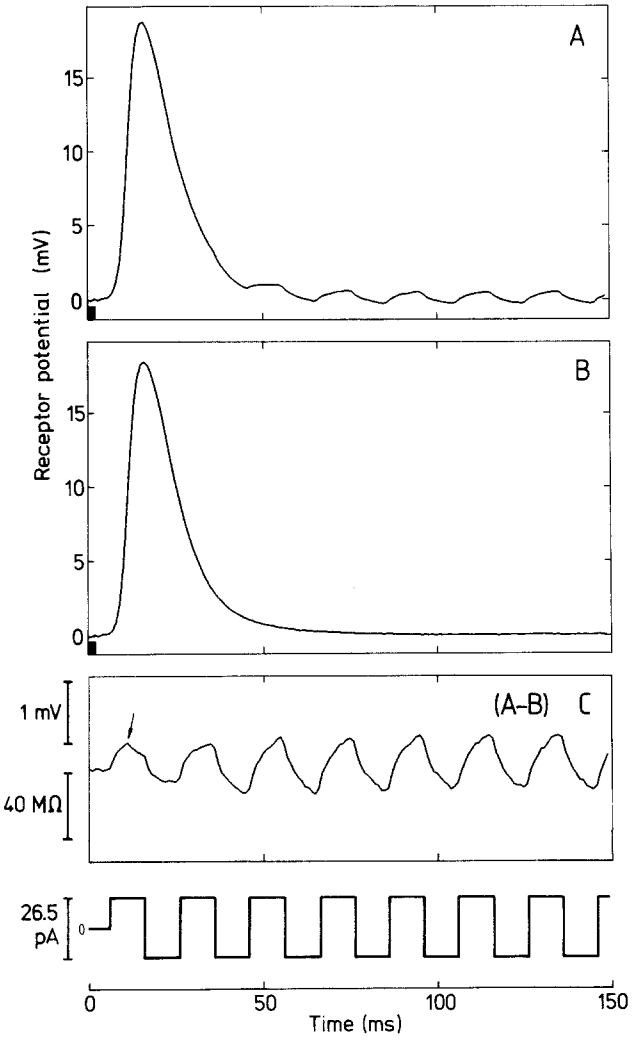

Fig. 11. **A** Response to a light flash (short bar, intensity 100, duration 2 ms) on all 6 neuro-ommatidial photoreceptor cells, combined with 10 ms current pulses of 13.3 pA, alternatively positive and negative (see lower trace); average of 1,280 responses. **B** Response to a light flash as in **A**, but without current pulses; average of 1,280 responses. **C** Difference of responses of **A** and **B**. The arrow indicates a sudden drop in input resistance of the cell in response to light

that the amplitude of the response has dropped significantly, as well as the time constant. The next (positive) current pulse, coinciding with the falling flank of the light response, shows the cell regaining its original input resistance and time constant, which are completely restored after a few more current pulses.

In a slightly different experiment (Fig. 12) a light flash was given (Fig. 12B), a steady current injected (Fig. 12C), and both together (Fig. 12A). Subtracting Fig. 12B and C from A results in Fig. 12D, that gives an impression of the cell's input resistance. We see that, contrary to the results of French and Kuster (1985) for the locust, the

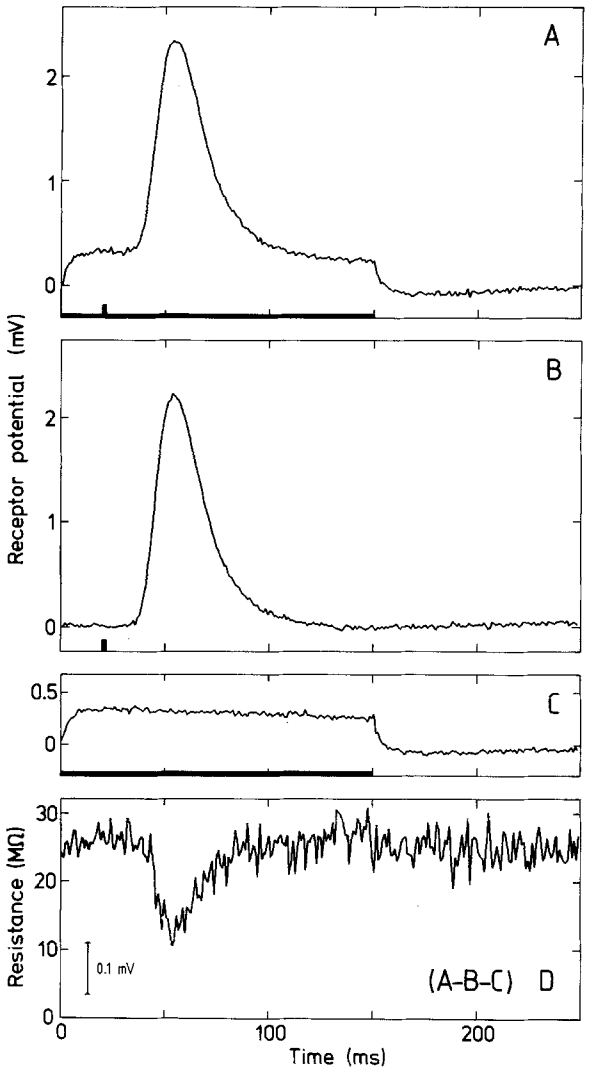

Fig. 12. **A** Response to a light flash (short bar, intensity 10, duration 2 ms) on all 6 neuro-ommatidial photoreceptor cells, combined with a 150 ms current pulse of 13.3 pA (long bar); average of 640 responses. **B** Response to the light flash of **A** without a current pulse; average of 640 responses. **C** Response to the current pulse of **A** without a light flash; average of 640 responses. **D** Responses of **B** and **C** subtracted from the response of **A**. The resistance follows from voltage and current, its value when the cell is not illuminated follows from **C**

input resistance of the cell changes in response to light. The interpretation of Fig. 12 is more complicated, however, than that of Fig. 11, because the input resistance and time constant can not be separated now, and interactions between photocurrent and injected current may not be negligible. Nevertheless, both experiments show that the electrical properties of the cell change appreciably during the response to light, even with responses of a few mV. This change in input resistance and time constant must be caused by a change in membrane resistance. This is not likely to be caused by the conductance change associated with the photocurrent: assuming the photocurrent to be mainly due to Na^+, assuming a driving potential of approximately 100 mV for Na^+, and assuming an input resistance of the cell of 30 MΩ (i.e. an input conductance of $33.10^{-9}\ \Omega^{-1}$), we conclude that a Na^+ conductance increase of $10^{-9}\ \Omega^{-1}$ produces a photocurrent of 0.1 nA, and a depolarization of 3 mV. Thus the conductance change necessary for a 3 mV depolarization is clearly negligible compared to the input conductance of the cell – the input conductance is probably mainly caused by the K^+ conductance. Although the change in membrane resistance we measured might in principle take place anywhere in the cell, we will argue in the Discussion that at least part of it occurs in the axon terminal of the photoreceptor.

Discussion

We will first present a model that explains the data, and that we will use for constructing the responses theoretically. Furthermore, we will discuss the consequences of the electrical coupling for the interpretation of some previous measurements on fly photoreceptors. Finally, we will examine the question of why these photoreceptors are coupled.

Towards a model

Figure 13 gives an overview of the theoretical model used (see also the Appendix). The T-network of Fig. 13A is an equivalent circuit for a cable segment, describing its input/output behaviour (see Appendix). Although photocurrent may enter the cell anywhere along the rhabdomere, we will make the approximation that current enters the cell only halfway along the cell body, be it photocurrent or current injected through a microelectrode. The cell can now be considered as consisting of 3 cable segments, two for the cell body and one for the axon (Fig. 13B, for an isolated cell). In Fig. 13B z_t is the impedance of the terminal. The input resistance R_{in} is defined as the quotient of the voltage in the cell body and the current injected in the cell body (v/i). R_1 is the input resistance of the cell as seen from the terminal, defined as the quotient of the voltage in the terminal and the current injected into the axon. The 6 neuro-ommatidial photoreceptor cells are coupled to their immediate neighbours in the ring of terminals by gap junction resistances R_g (Shaw 1984a), and by terminal impedances z_t to the lamina extracellular space, which is connected to the retina extracellular space by a barrier resistance R_b (see below). The complete

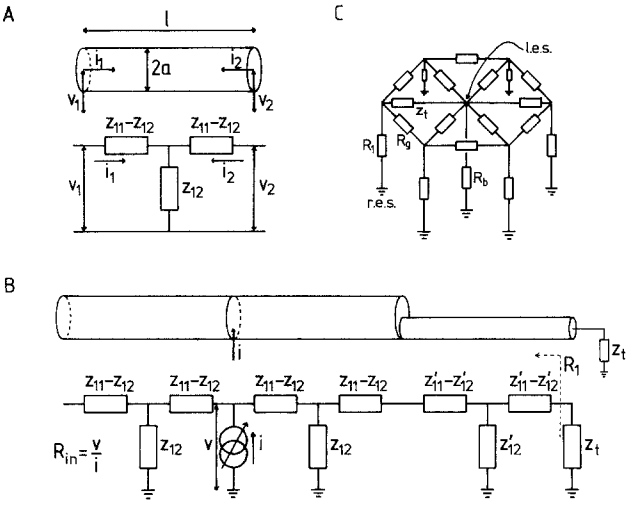

Fig. 13. **A** The input/output behaviour of a cable segment of length l and radius a is completely described by the T-circuit shown. Complex impedances z_{11} and z_{12} are given in the Appendix. **B** Model of an isolated cell modeled as consisting of 3 cable segments; current i enters halfway along the cell body. Impedances z_{11} and z_{12} are given in the text, primes denote impedances for the axon. R_{in} is the input resistance of the cell when measured in the cell body (defined as the quotient of the steady voltage v produced by a steady current i); R_l: input resistance of the cell as seen from the terminal; z_t: impedance of the terminal. **C** Model used for simulations described in this article. R_b: resistance of the barrier between retina and lamina; R_g: resistance of the gap junctions; z_t: impedance of the terminal; R_l: input resistance of a cell as seen from the terminal – if (photo)current was entering a cell the resistance R_l was replaced by the two-port model of **B**; l.e.s.: lamina extracellular space; r.e.s.: retina extracellular space

circuit is shown in Fig. 13C, where the resistances R_l represent the axons and cell bodies of the photoreceptor cells. Extracellular field potentials other than those in the lamina are neglected.

We have seen in Fig. 6 that the responses to illumination of 1 cell and 6 cells are different. With illumination of 6 cells, the responses of all cells are (approximately) equal, which also holds for the axon terminals. This means that in this case no current flows through the gap junctions (see Fig. 13C). In reality some current will flow, because the photoreceptors are not identically sensitive, and the cells and stimulus are inherently noisy (Laughlin and Lillywhite 1982), thus the cells will not give exactly equal responses. But the resulting current flowing through the gap junctions can be neglected compared to the current flowing in the case that only 1 cell is illuminated. In the latter case the illuminated cell is loaded by the gap junction resistances and the other cells in series with them (see Fig. 13C), and the input resistance of the cell is lower than it would be without this load. It seems likely that this extra load due to the gap junctions causes the fact that the responses are smaller when illuminating exclusively the recorded cell than when illuminating 6 cells.

Curve b of Fig. 6 (illumination of the recorded cell) is approximately linear (the deviations at higher flash intensities can be explained by self-shunting, see e.g. Matic and Laughlin 1981), whereas curve a (illumination of 6 cells) deviates more from linearity than curve b. This nonlinearity may have several causes. As a first cause, the transduction process might have a reduced yield for higher flash intensities, thus generating relatively less photocurrent than at low intensities. The input resistance of the cell might then remain virtually constant, apart from a negligible reduction due to light-dependent conductances (see Results). But there are two arguments against this possibility. First, we know from the experiments of Figs. 11 and 12 that the input resistance does not remain constant. Second, if only the transduction process generates relatively less photocurrent without other changes taking place, the curves a and b of Fig. 6 should have the same shape: the absence or presence of the load caused by the gap junctions only changes the input resistance of the cell, thus resulting in a scaling of curves a and b, but not in a difference in shape.

As a second cause of the nonlinearity of curve a in Fig. 6, the membrane resistance of some part of the cell might depend on the intensity of the light flash. This is suggested by Figs. 11 and 12. In this case the curves a and b of Fig. 6 are not expected to have the same shape, because the load caused by the gap junctions will be parallel to the load associated with the membrane resistance of the cell. If the load of the gap junctions is distinctly larger than the (changing) load caused by the membrane resistance of the cell, the resulting input resistance of the cell will remain virtually constant, thus the stimulus-response curve will be approximately linear (apart from self-shunting). This is exactly what we have found for illumination of one cell (Fig. 6, curve b). The load of the gap junctions is not present when 6 cells are illuminated, thus the curve will then be solely determined by the (changing) membrane resistance of the cell. This might cause the nonlinearity of Fig. 6, curve a. Of course, the first mentioned nonlinearity, due to the transduction process, might be present as well, but it can not explain the difference in shape between curves a and b in Fig. 6.

An interesting question is what part of the cell's membrane is changing its resistance in response to a light flash. Part of this change might occur in the cell body where it would function to shunt

the photocurrent. There are arguments, however, that at least part of this change occurs in the axons or terminals. Comparison of curves b and d in Fig. 6 (illumination of the recorded cell and one of its neuro-ommatidial neighbours) makes this plausible. These two curves should have the same shape as well, if the processes causing the change in the input resistance of the cell would only occur in the cell body: the efficiency of transfer of the signal from one cell to a neuro-ommatidial neighbour would not be affected. We see in Fig. 6, however, that the ratio of the curves b and d changes as a function of the light intensity. One of the simplest explanations of this phenomenon is that the resistance of the terminal (or axon, but see below) drops at higher flash intensities. This means that for higher flash intensities progressively more current flows into the lamina extracellular space instead of into the neighbouring neuro-ommatidial photoreceptor cells, which results in a lower coupling ratio. We will see below that an adapting terminal resistance would be a favourable mechanism for fast gain control.

A second possibility that would also explain the difference in shape between curves b and d of Fig. 6 is that the resistance of the gap junctions might increase as a function of flash intensity, also resulting in less current flowing into neighbouring neuro-ommatidial photoreceptor cells. But this possibility makes interpretation of curve b (illumination of the recorded cell) more difficult: an increasing resistance of the gap junctions reduces the load on the cell, thus increasing its input resistance. Consequently, curve b should not be approximately linear (apart from self-shunting), but should show higher peak response amplitudes than were measured at high flash intensities. Nevertheless, curve b is explained if we assume that an increasing resistance of the gap junctions is approximately compensated by a decreasing membrane resistance of the cell body. We will not pursue this possibility further, but assume for the sake of simplicity that only the terminal resistance changes.

Estimating the parameters

We will now first estimate the main parameters necessary for the model outlined above. First, we need the values of some of the properties of the cell, in particular the membrane resistance, the membrane capacitance, and the dimensions of the cell. We take for the membrane capacitance the standard value of 1 $\mu F/cm^2$, and for the intracellular resistivity 100 Ωcm (Jack et al. 1975). We assume a cylindrical cell body with a length of 250 μm, and a diameter of 5 μm (Wunderer and Smola 1982; Hardie et al. 1981). For the axon we assume a length of 35 μm, and a diameter of 2 μm. This does not include the part of the axon inside the neuro-ommatidium, which is defined here as the terminal of the cell.

We can now obtain the membrane resistance of the cell body by fitting a curve produced by the theoretical model to the measured curve of Fig. 10, where current was injected in the cell body. But there are two complications. First, the membrane area of the cell body is not only determined by its dimensions, but also by the area contributed by the microvilli in the rhabdomere. Second, the cell body can not be considered as an isolated part of the cell: the properties of the axon and axon terminal determine the cell's electrical properties as well. Moreover, the gap junctions at the terminal complicate these matters even further. We fitted a theoretical curve to the data in Fig. 10, assuming a gap junction resistance $R_g = 70$ MΩ and a terminal resistance $R_t = 1{,}000$ MΩ, assuming that the membrane resistance of the axon equals that of the cell body, and using the membrane resistance and the membrane area of the microvilli as parameters for fitting. This yielded a membrane resistance $R_m = 8$ kΩcm^2, and a membrane area of 35 μm^2 per μm length of the rhabdomere. If a smaller terminal resistance or gap junction resistance is assumed, the cell body is shunted more strongly, and a larger membrane resistance of the cell body has to be assumed to explain the cell's input resistance and time constant (for example, with a terminal resistance $R_t = 70$ MΩ a membrane resistance $R_m = 14$ kΩcm^2 is necessary to obtain a fit similar to that shown in Fig. 10). Current injection measurements in other cells could be fitted equally well, all yielding a membrane resistance of approximately 8 kΩcm^2, on assumption that most of the variability in input resistances and time constants was due to variations in the resistances of the gap junctions (Shaw 1984a) and variations in the membrane area in the rhabdomere (i.e. variations in the size of the rhabdomere). We will assume therefore in the following a membrane resistance $R_m = 8$ kΩcm^2.

The membrane area in the microvilli can also be estimated from the dimensions of the rhabdomere and the microvilli. Assuming a mean cross-sectional area of the rhabdomere of 1.6 μm^2, a mean distance between microvilli of 70 nm, a hexagonal packing, and a diameter of a microvillus of 45 nm (Hirosawa and Hotta 1982, for *Drosophila*), we estimate a membrane area of approximately 50 μm^2 per μm length of the rhabdomere

(see also Hardie et al. 1981, who estimated 70 $\mu m^2/\mu m$). These values are in reasonable agreement with the values determined from current injection experiments (approximately 40 $\mu m^2/\mu m$). It is worth emphasizing that the area of the membrane in the rhabdomere is more than 2 times as large as the remaining membrane area of the cell body (5π $\mu m^2/\mu m$), thus the rhabdomere is an important determinant of the cell's input resistance and capacitance (Hardie et al. 1981). Here we neglect possible complications caused by the close packing of the microvilli and the restricted extracellular space between the microvilli.

We assumed above that the membrane resistance of the axon was the same as that of the cell body. It is difficult to determine directly. Fortunately, the model calculations show that, unless this resistance is rather low (less than 200 Ωcm^2), the calculated responses are insensitive to varying it. The reason for this is the fact that the axon is short, and has an input resistance much higher than that of the cell body and presumably than that of the terminal. If the resistance is low (<200 Ωcm^2), the response to light is strongly attenuated when travelling from cell body to terminal, which is not consistent with the large coupling found from one cell body to a neuro-ommatidial neighbour. Nevertheless, it is possible that the membrane resistance of the axon drops in response to light, just as it is proposed here for the terminal resistance. We will not elaborate upon this possibility, but assume a membrane resistance of the axon similar to the membrane resistance of the cell body, i.e. $R_m = 8$ $k\Omega cm^2$.

The resistance of the gap junctions can be estimated from the coupling ratio between the cell bodies ($\sim 20\%$) and between the terminals ($\sim 50\%$). These ratios are produced by the theoretical model when the gap junction resistance is in the range of 10–50 MΩ. We will assume for the calculations a resistance of 25 MΩ. This is larger than the 2.5 MΩ that follows from estimates of the total area of the gap junctions between two terminals (0.4 μm^2, Shaw and Stowe 1982, but see also Shaw 1984a, who shows that this area varies from terminal pair to terminal pair) and the resistance of a gap junction (10^{-2} Ωcm^2, Loewenstein 1975). But the gap junction is likely to be somewhat closed because the terminal is about 10 mV positive to the lamina extracellular space (which is about 70 mV more negative than the retina extracellular space). This is also suggested by the fact that the photoreceptor cells are not dye-coupled by e.g. Lucifer yellow (Shaw and Stowe 1982).

The total membrane capacitance of the terminal follows from its dimensions and the standard value of 1 $\mu F/cm^2$ for membranes of nerve cells. We assume for the terminal a length of 20 μm, and a diameter of 2 μm. Assuming a longer length or an other diameter for the terminal does not change the calculations appreciably: the properties of the terminal are mainly determined by its resistance, which was estimated independently of the dimensions of the terminal. The resistance of the terminal follows in principle from the experiment where 6 cells are illuminated with flashes of various intensities. We assume that the aberrations from linearity are mainly caused by a change in terminal resistance (apart from self-shunting, which is included in the calculations). We will first try to estimate the terminal resistance for the lowest intensities. If it is lower than approximately 50 MΩ, our explanation of the linear behaviour of the intensity-response curve for illumination of only the recorded cell does not hold anymore: for the lowest intensities the terminal resistance should be distinctly larger than the gap junction resistance (assumed to be 25 MΩ). A terminal resistance larger than 1,000 MΩ, on the other hand, can already be considered as infinite: making it larger than 1,000 MΩ has no effect on the calculations. We will assume that for the lowest intensities a terminal resistance $R_t = 100$ MΩ is a reasonable estimate. From this we can find for the other intensities the terminal resistance that would produce the observed peak response amplitude (see also below).

Finally, the resistance barrier between retina and lamina must be taken into account, because this barrier probably causes the extracellular lamina depolarizations (Shaw 1975). From the amplitude of the lamina depolarizations a resistance $R_b = 2$ MΩ was estimated. Note that this is not the resistance per (neuro-)ommatidium, but that this also includes current pathways first going laterally through the lamina and then to the retina.

Model calculations

Examples of the model calculations are shown in Figs. 14 and 15. In Fig. 14 curves *a* (illumination of 6 cells) and *b* (illumination of 1 cell) were fitted to the measured points by adjusting the terminal resistance as a function of intensity, and approximating these terminal resistances R_t by the functions

$$R_t = 205.4/I^{0.75} \quad (1)$$

for curve a, and

$$R_t = 468.2/I^{0.75} \quad (2)$$

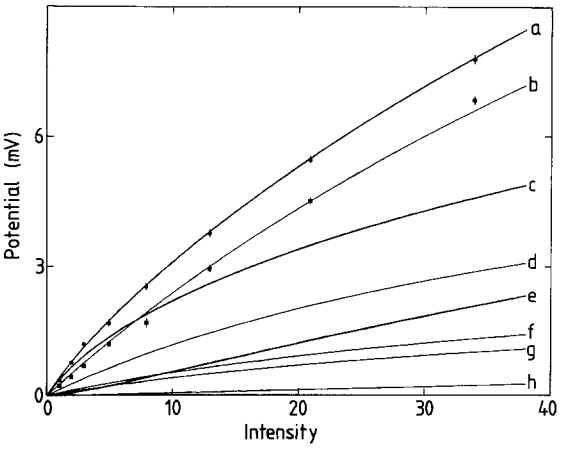

Fig. 14. Intensity-response curves obtained with the theoretical model outlined in the text. Experimental data from another cell than in Fig. 6. Stimuli as in Fig. 6. a: response in the cell body with illumination of 6 cells; b: response in the cell body of an illuminated cell; c: response in the axon terminal with illumination of 6 cells; d: response in the axon terminal of an illuminated cell; e: response in the lamina extracellular space with illumination of 6 cells; f: response in the axon terminal of the immediate neighbour of an illuminated cell; g: response in the cell body of the immediate neighbour of an illuminated cell; h: response in the lamina extracellular space with illumination of one cell. Parameters: membrane area of the rhabdomere: 40 $\mu m^2/\mu m$; membrane resistance of cell body and axon: 8 $k\Omega cm^2$; intracellular resistivity of cell body and axon: 100 Ωcm; membrane capacitance of cell body, axon, and terminal: 1 $\mu F/cm^2$; length of cell body: 250 μm, diameter: 5 μm; length of axon: 35 μm, diameter: 2 μm; length of terminal: 20 μm, diameter: 2 μm; resistance of gap junctions: 25 $M\Omega$; resistance of barrier between retina and lamina: 2 $M\Omega$; terminal resistance dependent on the intensity of the light flashes (duration 2 ms) as described in the text

for curve b, where I is the intensity of the light flash. These functions, which have only empirical meaning, were subsequently used for theoretical calculations of the peak response amplitudes at the cell body, terminal and lamina extracellular space, for various stimuli. Several features of the measurements are present in the theoretical curves: curve b (illumination of the recorded cell) is more linear than curve a (illumination of 6 cells), and their ratio is intensity dependent; the difference between illumination of 6 cells and 1 cell is larger in the terminal (curves c and d) than in the cell body (curves a and b); the coupling ratio between the cell bodies is about 20% (curves b and g), between the terminals about 50% (curves d and f, for next-neighbour terminals; the calculations yield a slightly smaller and slower coupling between cells further away from each other in the ring of terminals); for extracellular lamina depolarizations the difference between illumination of 6 cells (curve e) and 1 cell (curve h) is large. But there are also several differences between the measurements and the theoretical calculations: the intensity dependence of the coupling ratio between cell bodies (curves b and g) is stronger in the measurements (see Fig. 6) than in the model calculations; the intensity-response curves of the extracellular lamina depolarizations (curves e and h) are more linear in the calculations than in the measurements (see Fig. 9). Nevertheless, the overall agreement of experiment and theory is satisfactory.

The measurement of Fig. 15A (the same as in Fig. 14, 6 cells illuminated, intensity 13) was used for reconstructing other relevant potentials. In two cases, B and I, measurements were available as well (in I for an intensity of 10). Especially in Fig. 15I one of the insufficiencies of the model is clear: the response measured when a neuro-ommatidial neighbour is illuminated is generally broader (and with a shorter time to peak) than the theoretically predicted response (although this theoretical curve is already broader than the original measurement in Fig. 15A). This insufficiency probably arises from a simplification made in the calculations: it is assumed that the terminal resistance depends on the flash intensity, but does not change during the flash. This is clearly unrealistic (see Fig. 11), because whatever causes this change in terminal resistance (e.g. voltage sensitive conductances or feedback from secondary neurons), the adjustment will take some time, and may be a complicated function of voltage and time. A broadening of the depolarizations in the terminal and neighbouring photoreceptor cell could result if a voltage and time dependent terminal resistance is assumed: if we assume that the terminal resistance is lowest in the peak, as is suggested by Figs. 11 and 12, the response is more depressed in the peak than during the rising and falling flanks. This may also explain the fact that light flashes of higher intensity produce faster responses (Dubs 1981; but see French and Kuster 1985). A further possibility is that the terminal not only changes its resistance, but also actively produces membrane currents (see e.g. Koch 1984), as was found in rods in vertebrate eyes (Detwiler et al. 1978; Torre and Owen 1983). Although our measurements did not indicate such a mechanism, it can not be ruled out.

An interesting question is the time that a signal needs for going from the cell body to the terminal. We see in Fig. 15 (comparing B and E) that very little time is needed: the calculations give a delay of less than 200 μs. A delay of 2 ms as reported in the literature (Scholes 1969) must be considered doubtful; if present, it can not be explained by a delay caused by the cable properties of the axon.

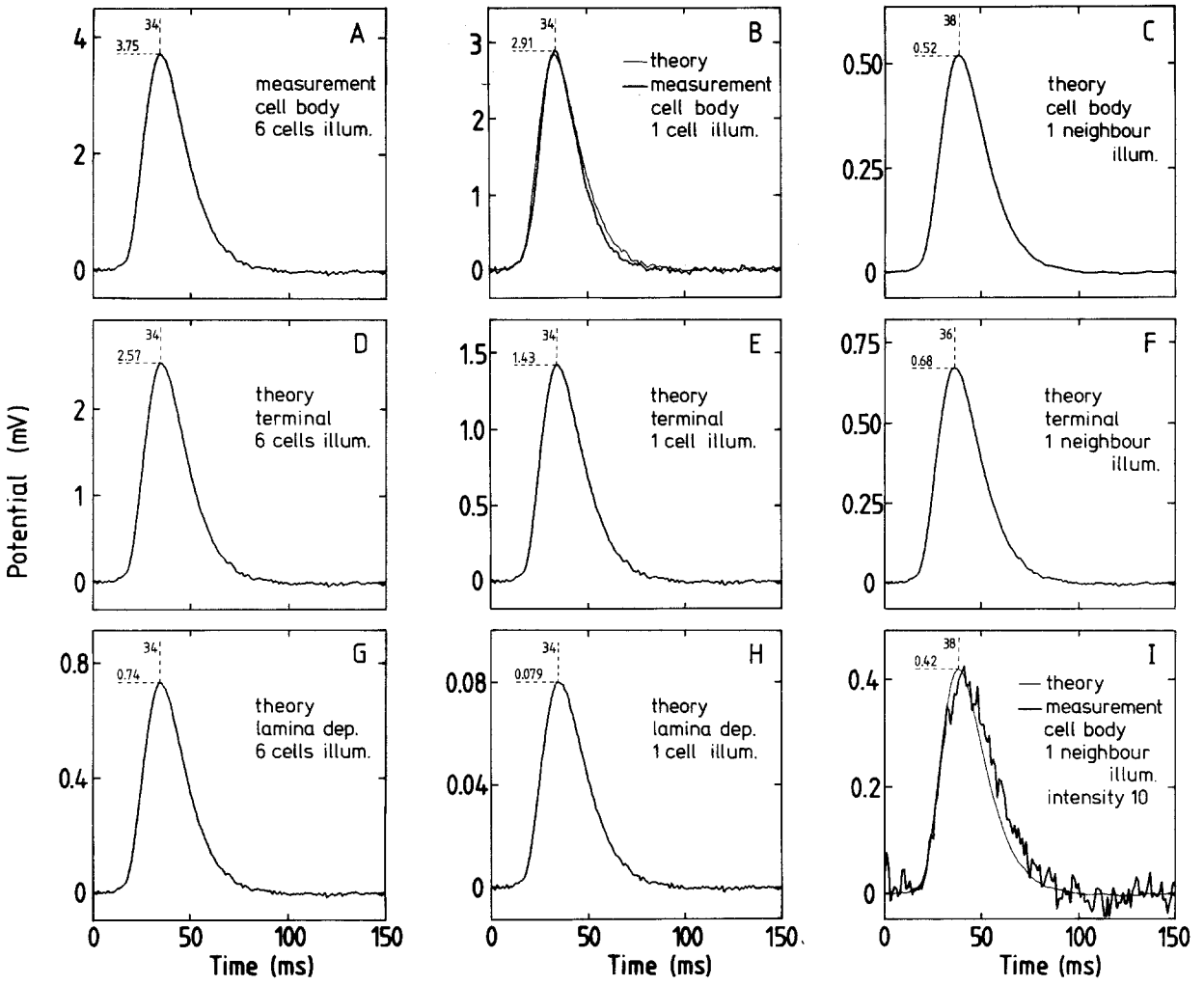

Fig. 15A–I. Examples of responses constructed with the theoretical model described in the text. Parameters as in Fig. 14, measurements from the same cell; intensity is 13 for all responses except **I**. Numbers near the peak of the responses: amplitude of the peak, and the time to peak. **A**, **D** and **G** Responses when 6 cells are illuminated, in **A** measured in the cell body, in **D** and **G** constructed from the response in **A** for the terminal and lamina extracellular space; **B** and **E** Responses in an illuminated cell, in **B** a measurement as well as a construction from the response in **A**; **C**, **F** and **I** Responses in an immediate neighbour from an illuminated cell, in **I** a measurement as well as a construction from the response in **A** for an intensity of 10. **H** Response in the lamina extracellular space when one cell is illuminated

Signal transport through the gap junctions and back to the cell bodies, however, is much slower (Fig. 15E, F and C), because the neighbouring cell body has to be charged by the current flowing through the gap junction and the axon, which takes time.

Consequences of coupling

Before going into some speculations as to why the gap junctions are present, and why the terminal resistance would change, we will first discuss some of the consequences of the coupling for measurements that have traditionally been performed on the fly's visual sense cells, in particular the angular sensitivity, bumps, spectral and polarization sensitivity. This is an important matter, because although virtually all measurements were done by illuminating 6 cells, it has often been assumed that the response could be interpreted as only coming from the recorded cell. Because we have seen that this view is incorrect, we have to reexamine previous measurements.

Figure 16 shows an angular sensitivity measured in various ways (for details see van Hateren 1984, 1985, and Smakman et al. 1984). In one of these measurements all photoreceptors looking into the same direction were illuminated, in the other two measurements only the ommatidium with the recorded photoreceptor cell was illumi-

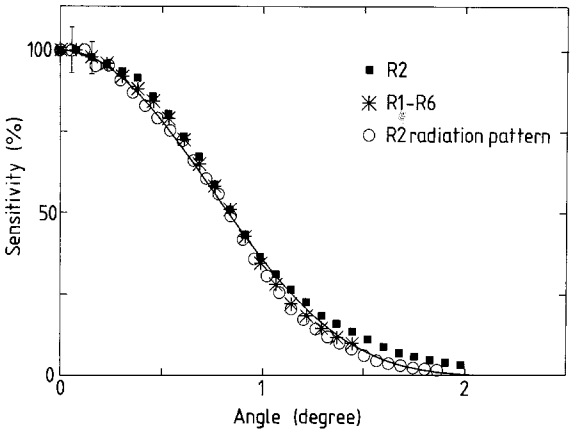

Fig. 16. Angular sensitivity of an R2 measured in various ways. Circles show the angular sensitivity measured from the radiation pattern of R2 photographed in the far field and evaluated by means of microdensitometry. Filled squares: the angular sensitivity measured electrophysiologically (by clamping the response to light flashes to a steady value by feedback of the receptor potential to the light intensity) with illumination of only the ommatidum that contains R2 (other ommatidia are shielded off with a diaphragm). Asterisks: the angular sensitivity measured electrophysiologically with illumination of all cells looking into the same direction as the R2 impaled. The continuous curve is a theoretical prediction of the angular sensitivity using a model based on waveguide theory. Diameter of the facet lens 24.5 μm, wavelength 600 nm (using filter K60, Balzers). (For details, see van Hateren 1984, 1985)

nated (by shielding off the other ommatidia with a diaphragm). We see that the shape of the angular sensitivity is not significantly different for illumination of 1 cell or 6 cells (the responses with illumination of 6 cells were slightly larger, however). This is to be expected, because the 6 coupled photoreceptors look into the same direction and thus all contribute equally to the resulting angular sensitivity. From optical measurements Pick (1977) concluded that the visual axes of the 6 cells point in slightly different directions. However, this difference does not really broaden the angular sensitivity: the superposition of 6 Gaussian curves (as approximations of the angular sensitivities) is less than 5% broader than the composing curves if the distances between the centres of the curves are less than 20% of their half-width. This condition is generally fulfilled in the eye of the blowfly.

In Fig. 17A spontaneous bumps (responses to single photons) are shown for continuous illumination of the recorded cell, and in Fig. 17B of the 6 coupled cells. With illumination of 6 cells we can see, in addition to large bumps of about 2 mV, many smaller bumps (e.g. see arrows), which are somewhat broader than the large bumps. These smaller bumps are presumably bumps from neigh-

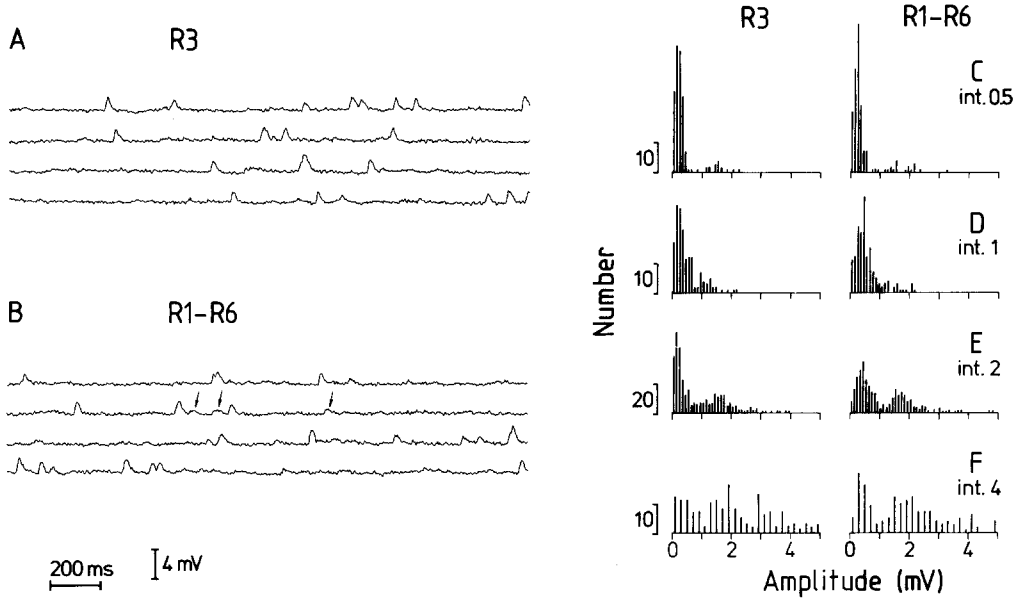

Fig. 17. **A** Spontaneous bumps in response to continuous illumination (intensity 0.1) of a recorded R3. **B** Spontaneous bumps in response to continuous illumination of all the neuro-ommatidial cells belonging to the R3 of **A**. Apart from large bumps of about 2 mV, there are also small bumps: examples are indicated by arrows. Traces sampled at 1 kHz, and mildly filtered afterwards by a running mean of 5 ms. **C**, **D**, **E** and **F** Amplitude distribution of responses to light flashes (duration 2 ms, intensity indicated in the figures) for illumination of R3 and R1–R6 (same cells as in **A** and **B**). The amplitude was determined by subtracting the mean response in the interval between 200 and 250 ms after the flash from the maximum response in the interval between 30 and 70 ms after a light flash; both calculated on a signal sampled at 1 kHz and filtered afterwards by a running mean of 5 ms. With illumination of 6 cells, there is, in addition to a peak at an amplitude of about 2 mV, another peak at about 0.3 mV. The latter presumably arises from bumps in neuro-ommatidial cells other than R3. The peak near 0 mV, present with illumination of the recorded cell as well as with illumination of 6 cells, arises from noise

bouring neuro-ommatidial sense cells that are transmitted through the gap junctions. In a slightly different experiment small flashes of low intensity were given, eliciting sometimes a bump, and sometimes not. Figure 17C, D, E and F show the amplitude distributions of the responses for various flash intensities and for illumination of 1 cell and 6 cells. Here there are also differences, which are best seen in Fig. 17E (intensity 2). When illuminating 6 cells there is, apart from a peak at about 2 mV, a second peak at about 0.3 mV, again interpreted as being caused by bumps in neuro-ommatidial neighbours (cf. Dubs et al. 1981).

Spectral sensitivities are not influenced by the coupling, because R1–R6 have similar spectral sensitivities. This is not the case, however, for polarization sensitivities (defined as maximum sensitivity/minimum sensitivity). Taking only coupling between direct neuro-ommatidial neighbours into account (coupling ratio 20%), assuming that their polarization axes are at 60 ° at each other (Hardie 1984), and assuming linearity (which is only approximately true for small intensities), we find

$$PS_1 = \frac{1.1\,PS_6 - 0.3}{1.1 - 0.3\,PS_6} \qquad (3)$$

where PS_6 is the polarization sensitivity for illumination of 6 cells, and PS_1 for illumination of the recorded cell. Taking $PS_6 = 2$ (Hardie 1984) yields $PS_1 = 3.8$. Moreover, PS_6 will depend on intensity. The fact that PS_6 varies from cell to cell (Hardie 1984) may be partially due to variations in the area – and thus the resistance – of the gap junctions (Shaw 1984a).

Why coupling?

Finally we will go into some speculations as to why the system is built as proposed here. First, we may wonder why the terminal resistance would change. One reason may be that it functions as a fast gain control, controlling the amplitude and time course of the input to the synapses to second order neurons. Although a gain control by conductances that shunt the photocurrent is likely also present in the cell body, it can act faster and more efficiently at the terminal, close to the synapses. Furthermore, even if this shunting terminal resistance becomes very small, the load on the cell body – and thus the current drawn from it – remains limited, because the axon isolates the terminal somewhat from the cell body. Another advantage of the terminal as a site of gain control, is that it is well accessible to second and higher order neurons that may be involved in regulating light adaptation; also neuromodulators and neurohormones can easily reach the terminals.

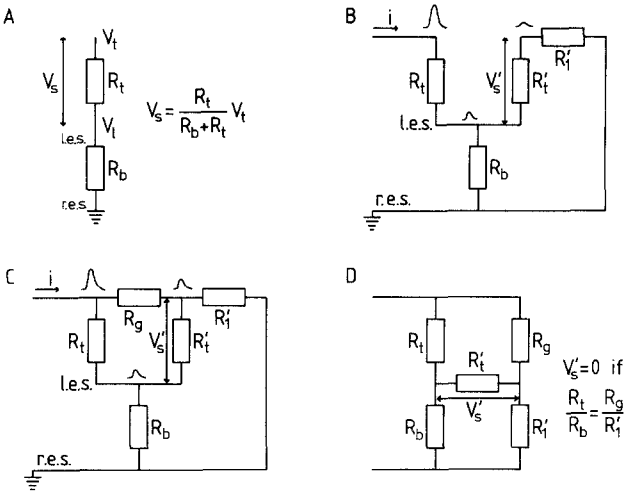

Fig. 18. **A** The terminal resistance R_t functions together with barrier resistance R_b as a voltage divider. V_s: potential over the terminal membrane. V_t: terminal potential, V_l: potential of the lamina extracellular space (l.e.s.), r.e.s.: retina extracellular space. **B** Depolarizations of: lamina extracellular space may cause inhibition in nearby cells. R_t: terminal resistance of the illuminated cell, R_t': terminal resistance of the other cell, R_b: resistance of the barrier between retina and lamina, V_s': potential over the membrane of the second cell, R_t': input resistance of the second cell as seen from the terminal. **C** Same as **B**, but now with a gap junction resistance R_g, which may offset the inhibition caused by the extracellular field potentials. **D** Same as **C**, but rearranged to show that it is a bridge circuit, with the terminal resistance of the second cell forming the bridge. The potential V_s that the synapse of the second cell experiences can be made zero, positive or negative by appropriate choices of the resistances involved

The terminal as a site of gain control is made even more effective by the resistance barrier between retina and lamina (Shaw 1975). This can be best understood from the simplified scheme in Fig. 18A. The terminal resistance and barrier resistance act together as a voltage divider. Therefore, the gain is small if the terminal resistance is small compared to the barrier resistance. Moreover, the barrier acts in cooperation with the axon as a current limiter, delimiting the load on the cell body.

The gap junctions present us with another intriguing question: why are those cells coupled, that anyhow superpose at the second order neurons? Ribi (1978) argued that presynaptic averaging might be useful to smooth large fluctuations that would be amplified by the nonlinear synapse. An alternative explanation is the following. To simplify matters we will first look at only two photoreceptor cells. Suppose that no gap junction would be present (Fig. 18B). Then illumination of one cell would cause the depolarizations shown in the figure: a relative large response in the terminal of

the illuminated cell, a smaller extracellular depolarization, and an even smaller response in the terminal of the other cell. The voltage that the synapse of this cell sees, is then negative, thus the synapse is inhibited (Shaw 1975). Now suppose that there are gap junctions (Fig. 18C). Then illumination of one cell would cause a larger depolarization in the terminal of the other cell than without gap junctions, because current flows through the gap junctions. Rearranging Fig. 18C leads to Fig. 18D, which is readily recognized as a bridge circuit. The synapse of the second cell constitutes the bridge. The synaptic voltage can now be made zero by choosing appropriate values for the resistances involved (see figure).

We thus reach the surprising conclusion, that gap junctions may be used to decouple two cells instead of coupling them. Depending on the exact values of the resistances involved, two neighbouring cells can excite each other, inhibit each other, or be completely independent. If more than 2 cells are coupled, e.g. 6 as in the neuro-ommatidia of the fly, the situation is more complicated. Although the cells can not be completely decoupled now, the coupling can be reduced appreciably by the gap junctions. From the measurements presented in this article, it seems that the system in the fly is tuned so that the terminals excite each other substantially with light flashes of low intensity, and less with flashes of higher intensity, but more precise measurements are necessary to settle the question, e.g. double recordings from photoreceptor terminals and extracellular lamina depolarizations. It is of course well possible, that the tuning depends on the state of light adaptation of the cells, be it by adjustment of the terminal resistance, of the gap junction resistance, or of the barrier resistance (this would occur for example if the glial cells vary the lateral resistance in the lamina).

Conclusion

One of the major findings presented in this article is that fly photoreceptor cells are not isolated entities, but are part of a complex neuropil. This parallels findings in the vertebrate retina (e.g. the rod network in the salamander retina, Atwell et al. 1984). Therefore, we must exercise great care when ascribing the responses of photoreceptor cells exclusively to the recorded cell. Of course, this proviso most probably also applies to other neurons.

The method of microstimulation using water-immersion has been shown in this article to be a most valuable tool for studying the coupling of the photoreceptor cells. Especially for the study of second and higher order neurons it promises to be an equally powerful method.

Acknowledgements. I wish to thank Doekele Stavenga for stimulating discussions and critical comments on the manuscript, Rob de Ruyter for his stimulating interest in this work, Diek Duifhuis for useful suggestions concerning cable theory, Jan Kuiper for his support to this work, Enno Nienhuis and Udo Douma for their expert technical assistance, Ben Pijpker for his expertise in electronics, Eric Bosman for software support, and Henk Zaagman for excellent advise on computer matters. This research was partially supported by the Dutch Organization for the Advancement of Pure Research (Z.W.O.) through the Foundation for Biophysics.

Appendix

The T-network shown in Fig. 13A completely describes the input/output behaviour of a cable segment (see van Hateren 1986). The complex impedances z_{11} and z_{12} are given by (see also Koch and Poggio 1985)

$$z_{11}=\frac{z_a}{g}\frac{\exp(lg)+\exp(-lg)}{\exp(lg)-\exp(-lg)} \tag{4}$$

$$z_{12}=\frac{z_a}{g}\frac{2}{\exp(lg)-\exp(-lg)}, \tag{5}$$

with l the length of the cable segment, and

$$g=\left(\frac{z_a}{z_m}\right)^{\frac{1}{2}}, \tag{6}$$

and

$$z_a=r_a=\frac{R_a}{\pi a^2} \tag{7}$$

$$z_m=\left(\frac{1}{r_m}+i\omega c_m\right)^{-1}=\left(\frac{2\pi a}{R_m}+i\omega 2\pi a C_m\right)^{-1}, \tag{8}$$

where a is the radius of the cable segment, R_a the intracellular resistivity (taken to be 100 Ωcm), R_m the membrane resistance, and C_m the membrane capacitance (taken to be 1 $\mu F/cm^2$). The circuit is completely defined by Fig. 13C, so all voltages and currents can be constructed given some measured voltage or current. Measurements in the time domain are first transformed with a fast Fourier transform to the frequency domain, then multiplied by the proper transfer function determined from the circuit, and finally transformed back to the time domain. Practical ways to handle this circuit are treated elsewhere (van Hateren 1986).

References

Attwell D, Wilson M, Wu SM (1984) A quantitative analysis of interactions between photoreceptors in the salamander (*Ambystoma*) retina. J Physiol 352:703–737

Chi C, Carlson SD (1976) Close apposition of photoreceptor cell axons in the house fly. J Insect Physiol 22:1153–1157
Detwiler PB, Hodgkin AL, McNaughton PA (1978) A surprising property of electrical spread in the network of rods in the turtle's retina. Nature 274:562–565
Dubs A (1981) Non-linearity and light adaptation in the fly photoreceptor. J Comp Physiol 144:53–59
Dubs A, Laughlin SB, Srinivasan MV (1981) Single photon signals in fly photoreceptors and first order interneurons at behavioural threshold. J Physiol 317:317–334
Franceschini N (1975) Sampling of the visual environment by the compound eye of the fly: Fundamentals and appli cations. In: Snyder AW, Menzel R (eds) Photoreceptor Optics. Springer, Berlin Heidelberg New York, pp 98–125
French AS, Kuster JE (1985) Nonlinearities in locust photoreceptors during transduction of small numbers of photons. J Comp Physiol A 156:645–652
Hardie RC, Franceschini N, Ribi W, Kirschfeld K (1981) Distribution and properties of sex-specific photoreceptors in the fly *Musca domestica*. J Comp Physiol 145:139–152
Hardie RC (1984) Functional organization of the fly retina. In: Ottoson D (ed) Progr sensory physiol, vol 5. Springer, Berlin Heidelberg New York Tokyo, pp 1–79
Hateren JH van (1984) Waveguide theory applied to optically measured angular sensitivities of fly photoreceptors. J Comp Physiol A 154:761–771
Hateren JH van (1985) The Stiles-Crawford effect in the eye of the blowfly, *Calliphora erythrocephala*. Vision Res 25:1305–1315
Hateren JH van (1986) An efficient algorithm for cable theory, applied to blowfly photoreceptor cells and LMC's. Biol Cybern (in press)
Hirosawa K, Hotta Y (1982) Morphological analysis of photoreceptor membranes in mutant *Drosophila* eyes. In: Hollyfield JG (ed) The structure of the eye. Elsevier North Holland, Amsterdam, pp 45–53
Jack JJB, Noble D, Tsien RW (1975) Electric current flow in excitable cells. Clarendon Press, Oxford
Kirschfeld K, Franceschini N (1968) Optische Eigenschaften der Ommatidien im Komplexauge von *Musca*. Kybernetik 5:47–52
Koch C (1984) Cable theory in neurons with active, linearized membranes. Biol Cybern 50:15–33
Koch C, Poggio T (1985) A simple algorithm for solving the cable equation in dendritic trees of arbitrary geometry. J Neurosci Meth 12:303–315
Laughlin SB, Lillywhite PG (1982) Intrinsic noise in locust photoreceptors. J Physiol 332:25–45
Loewenstein WR (1975) Permeable junctions. In: Cold Spring Harbour Symp Quant Biol XL:49–63
Matic T, Laughlin SB (1981) Changes in the intensity-response function of an insect's photoreceptor due to light adaptation. J Comp Physiol 145:169–177
Muijser H (1979) A micro-electrode amplifier with an infinite resistance current source for intracellular measurements of membrane potential and resistance changes under current clamp. Experientia 35:912–913
Pick B (1977) Specific misalignments of rhabdomere visual axes in the neural superposition eye of dipteran flies. Biol Cybern 26:215–224
Ribi WA (1978) Gap junctions coupling photoreceptor axons in the first optic ganglion of the fly. Cell Tissue Res 195:299–308
Scholes J (1969) The electrical responses of the retinal receptors and the lamina in the visual system of the fly *Musca*. Kybernetik 6:149–162
Shaw SR (1975) Retinal resistance barriers and electrical lateral inhibition. Nature 255:480–483
Shaw SR (1981) Anatomy and physiology of identified nonspiking cells in the photoreceptor-lamina complex of the compound eye of insects, especially Diptera. In: Roberts A, Bush BMH (eds) Neurons without impulses. Cambridge University Press, Cambridge, pp 61–116
Shaw SR (1984a) Asymmetric distribution of gap junctions amongst identified photoreceptor axons of *Lucilia cuprina* (Diptera). J Cell Sci 66:65–80
Shaw SR (1984b) Early visual processing in insects. J Exp Biol 112:225–251
Shaw SR, Stowe S (1982) Freeze-fracture evidence for gap junctions connecting the axon terminals of dipteran photoreceptors. J Cell Sci 53:115–141
Smakman JGJ, Hateren JH van, Stavenga DG (1984) Angular sensitivity of blowfly photoreceptors: intracellular measurements and wave-optical predictions. J Comp Physiol A 155:239–247
Smakman JGJ (1985) Angular and spectral sensitivity of blowfly photoreceptors. Thesis, Groningen University
Torre V, Owen WG (1983) High-pass filtering of small signals by the rod network in the retina of the toad, *Bufo marinus*. Biophys J 41:305–324
Wunderer H, Smola U (1982) Morphological differentiation of the central visual cells R7/8 in various regions of the blowfly eye. Tissue Cell 14:341–358